BB

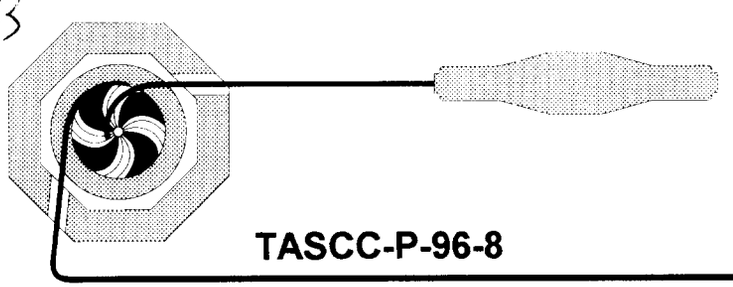

PREPRINT

tascc

TASCC-P-96-8

PIONIC FUSION OF HEAVY IONS

D. Horn[1], G.C. Ball[1], L. Beaulieu[2], D.R. Bowman[1], W.G. Davies[1], D. Fox[1], A. Galindo-Uribarri[1], A.C. Hayes[1], Y. Larochelle[2], C. St-Pierre[2], and G. Savard[1]

1 *AECL, Chalk River Laboratories, Chalk River, ON K0J 1J0, Canada*
2 *Laboratoire de physique nucléaire, Département de physique, Université Laval, Ste-Foy, QC G1K 7P4, Canada*

Advances in Nuclear Dynamics: Proceedings of the 12th Winter Workshop on Nuclear Dynamics

Physical and Environmental Sciences
Chalk River Laboratories
Chalk River, ON K0J 1J0 Canada

1996 April

PIONIC FUSION OF HEAVY IONS

D. Horn,[1] G.C. Ball,[1] L. Beaulieu,[2] D.R. Bowman,[1] W.G. Davies,[1] D. Fox,[1] A. Galindo-Uribarri,[1] A.C. Hayes,[1] Y. Larochelle,[2] C. St-Pierre,[2] and G. Savard[1]

[1]AECL, Chalk River Laboratories, Chalk River, ON, Canada K0J 1J0
[2]Laboratoire de physique nucléaire, Département de physique, Université Laval, Ste-Foy, QC, Canada G1K 7P4

INTRODUCTION

The previously unobserved phenomenon of heavy-ion pionic fusion is the ideal tool for investigation of coherent mechanisms of pion production, since it is the only pionic channel open very near absolute threshold, where the contribution from on-shell nucleon-nucleon mechanisms is the smallest. We begin this paper with a discussion of the existing data on heavy-ion pion production at low energies and review the models intended to provide the requisite coherent pion production mechanisms. We then present our measurement of the ^{12}C(^{12}C,^{24}Mg)π^0 and ^{12}C(^{12}C,^{24}Na)π^+ cross sections at E_{cm} = 137 MeV, which is an order of magnitude closer to threshold than the energy of earlier, inclusive heavy-ion measurements. This constitutes the first experimental observation of the pionic fusion of heavy ions and places severe constraints on the pion production mechanisms. We discuss the impact of this finding on the proposed models, which must now incorporate the kinetic energy of the entire 24-nucleon system as well as the binding energy gained in fusion.

PION PRODUCTION IN LOW-ENERGY HEAVY-ION REACTIONS

Figure 1 is a schematic representation of a heavy-ion reaction in which a pion is produced. The entrance channel is defined by the projectile and target nuclei and their center-of-mass energy, and the final state may be measured experimentally. The goal of experiments and calculations in this field is to find a production mechanism which satisfies all known aspects of the initial and final states and links the two in a physically reasonable model. See Cassing *et al.*[1] for a review of recent progress in this field. Reactions in which the available energy substantially exceeds the total pion relativistic

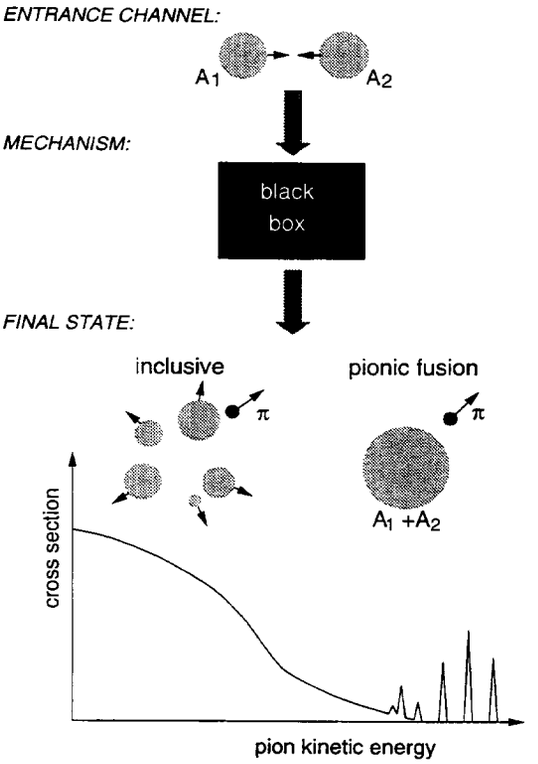

Figure 1. Heavy-ion pion production. The many-body (lower left) and pionic fusion (lower right) final states contribute to the low-energy and high-energy parts of the pion spectrum, respectively.

mass generally result in many-body final states with a continuum of pion energies[2]. If, however, there is little excess energy, a bound nucleus may be formed which does not decay by nucleon or cluster emission; the pion energy spectrum would then reflect discrete levels in the fused nucleus. This phenomenon has previously been observed in light-ion reactions[3]-[5]. In such a pionic fusion reaction, measurement of either the pion or the heavy residue consitutes a kinematically complete characterization of the binary exit channel.

An extensive set of inclusive π^0 cross-section measurements is tabulated by Prakash *et al.*[6], but the lowest-energy experiment quoted there[7] has a center-of-mass energy of nearly twice the pion mass. Closer to absolute threshold, sub-nanobarn cross sections make measurements very difficult, since pion detection is generally inefficient and subject to high backgrounds.

From the rather energetic reactions measured in the 1980s, it was already evident that that models based upon on-shell nucleon-nucleon production mechanisms, even with the inclusion of the intrinsic nucleon Fermi motion[8], could not reproduce the lower-energy pion cross sections[1]. New models incorporating cooperative mechanisms via "pionic bremsstrahlung"[9] and statistical compound-nucleus emission of pions[6, 10] were proposed for heavy-ion reactions. Fully quantum-mechanical treatments were initially reserved for proton-induced reactions[11], and later extended to ^{3}He-induced reactions[12]. Typically they involved a primary nucleon-nucleon pion production mechanism, an amplitude for rescattering this virtual pion on-shell, and a nuclear structure form factor.

To test these models it was therefore desirable to measure reactions very near

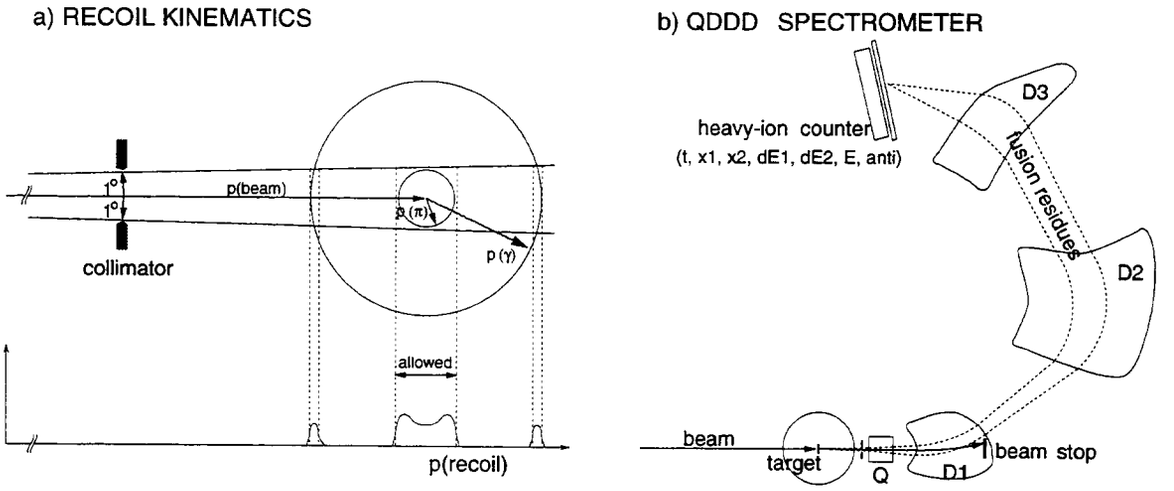

Figure 2. Kinematics and spectroscopy of pionic fusion residues. a) Momentum loci of A=24 residues, after emission of a pion and after emission of a high-energy γ-ray. A one-dimensional momentum spectrum is projected for ions passing a one-degree collimator. b) Diagram of the experimental setup, showing the QDDD spectrometer magnetic elements, focal-plane detector, internal beam stop, and collimation.

threshold, where all pion production channels with the exception of pionic fusion would be closed. While this imposes the difficulty of very low cross sections, it does offer an alternative to the inefficient direct detection of pions: the fusion residues are detectable with high efficiency, as they are well localized in momentum space; they are easily identifiable, and should be unambiguous indicators of pion production. Any ^{24}Mg compound nucleus formed without emitting a high-energy quantum, such as a pion or a bremsstrahlung photon, should decay by nucleon or cluster emission, giving a mass less than 24; high-energy photon emission can be excluded kinematically by the large momentum it transfers to the recoil (See Fig. 2a). Accordingly, we chose to detect the mass-24 fusion products of the ^{12}C(^{12}C,^{24}Mg)π^0 and ^{12}C(^{12}C,^{24}Na)π^+ reactions, rather than the pions themselves.

EXPERIMENT

A ^{12}C beam of $E_{lab} = 274.2 \pm 1.2$ MeV from Chalk River's TASCC facility was incident on an isotopically separated ^{12}C target of 826 μg/cm^2 areal density. The target was prepared with precautions to minimize contamination, baked in a vacuum oven, and stored and transferred in an inert atmosphere. With the assumption of a maximum-energy 6-MeV pion emitted transversely and with allowance for multiple scattering in the target, the ^{24}Na and ^{24}Mg products recoil within one degree of the beam axis. We therefore aligned the Chalk River QDDD spectrometer[13] at $\theta_{lab} = 0°$, as shown in Fig. 2b, and collimated its entrance with a circular aperture of 1 msr solid angle, corresponding to a cone of 1° half-angle. The carbon beam was stopped and current-integrated on a beam block positioned inside the spectrometer's magnet box; cleanup of scattered beam was provided by a scraper paddle placed further into the spectrometer. Ions with the appropriate momentum-to-charge ratio were deflected to the spectrometer's focal plane and registered in a heavy-ion counter[14], providing measurements of the time, position, energy-loss, energy and punch-through rejection as indicated in the figure. Events electronically imitating mass-24 recoil signals, such

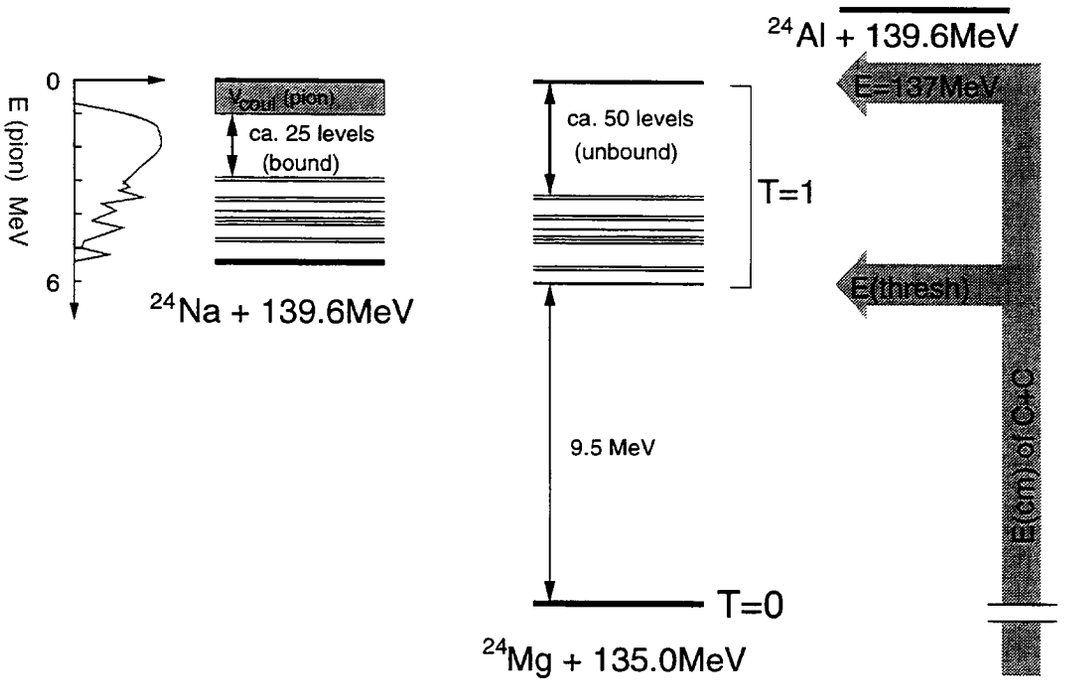

Figure 3. Energetics of the $^{12}C+^{12}C$ pionic fusion reaction at E_{cm} = 137 MeV. The reaction is subthreshold for the $^{24}Al+\pi^-$ exit channel, and about 6 MeV above threshold for the other two channels. The (center-of-mass) pion energy spectrum corresponding to the excited states of the residue is shown schematically on the right.

as several ions reaching the counter at nearly the same time, were largely eliminated by timing, pileup rejection, and anticoincidence requirements. The momentum calibration was obtained from the position signals produced with a 138-MeV ^{24}Mg beam for various spectrometer magnetic fields. The charge-state distributions for 120- to 150-MeV ^{24}Mg ions exiting a carbon target were measured (more than half were fully stripped) and the results extrapolated for sodium.

The energetics of the pionic reaction channels are illustrated in Fig. 3. The $^{12}C(^{12}C,^{24}Al)\pi^-$ channel is forbidden by energy conservation. Since the carbon nuclei in the entrance channel are in T=0 states, production of a T=1 pion in a binary exit channel requires that the fusion residue be left in a T=1 state. While low-lying states in ^{24}Na are of this type, the lowest-lying T=1 state in ^{24}Mg is at 9.5 MeV of excitation, raising the absolute threshold for the reaction to E_{cm} = 131 MeV. The velocity spectra for ^{24}Mg and ^{24}Na should then be centered on the reaction center-of-mass velocity with a width defined by the recoil from emission of a pion of 6 MeV or less; additional broadening of the measured spectra would arise from energy loss in the target material and from resolution effects.

RESULTS

Recoil velocity spectra

Recoil velocity spectra for ^{24}Na and ^{24}Mg are shown in Fig 4. The open symbols represent galilean-invariant yields, corrected for dead time and counter efficiency and the error bars are based on counting statistics. Double-ended arrows indicated the

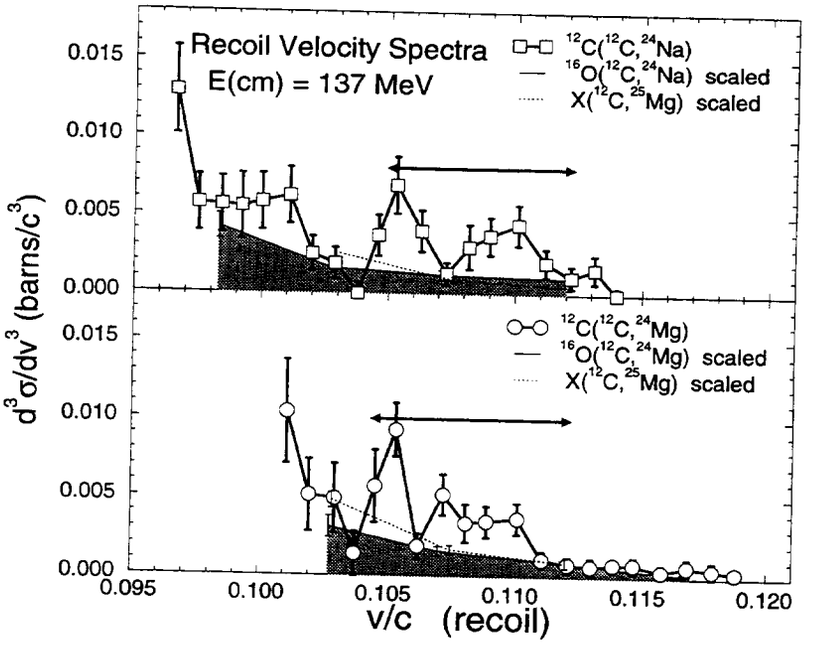

Figure 4. Galilean-invariant cross sections as a function of recoil velocity, obtained with the 826-μg/cm^2 target, for the reactions ^{12}C(^{12}C,^{24}Na) (squares, top panel) and ^{12}C(^{12}C,^{24}Mg) (circles, bottom panel) at E_{cm} = 137 MeV. The double-headed arrows indicate the expected width of the recoil velocity distributions from the π^+ (top) and π^0 (bottom) pionic fusion reactions. The shaded regions represent the measured A=24 yields from the ^{12}C+^{16}O reaction, scaled to represent the background due to oxygen contamination of the target; the dotted line is an alternative background determination based on ^{25}Mg yields.

expected widths of the velocity distributions as defined above; based on a combination of uncertainties in calibration, beam energy, and energy-loss straggling in the target, the absolute uncertainty in the placement of these ranges relative to the velocity axis is 0.0005c. While there is a clear enhancement in the yield of mass-24 residues at the expected velocities, the cross section outside the "allowed" velocity region is not zero. Note, in particular, the rise in yield toward velocities well below the center-of-mass velocity for the ^{12}C +^{12} C system, as would be characteristic of evaporation residues from reactions with contaminants heavier than carbon.

Background Considerations

The presence of ^{24}Na and ^{24}Mg ions from reactions with target contaminants necessitated a detailed examination of background yields. An elastic recoil detection (ERD)[15] analysis of the target composition revealed oxygen to be present at the 1% level; a smaller amount of aluminum was also observed. Rather than interpolate the background level in the "allowed" velocity range from measurements on either side of it, we explicitly measured the ^{16}O(^{12}C,^{24}Na) and ^{16}O(^{12}C,^{24}Mg) yields from a 150-μg/cm^2 MoO_2 target. Normalization to the carbon-target data was done by reproducing the mass-23 yields in the velocity range of interest, since the main source of that mass is target contamination (single-nucleon emission from the composite A=24 system is so energetic that momentum conservation ejects the mass-23 recoil from the velocity region of interest). The shaded regions in Fig. 4 represent the background due to oxygen contamination of the target. An alternative background calculation (dashed

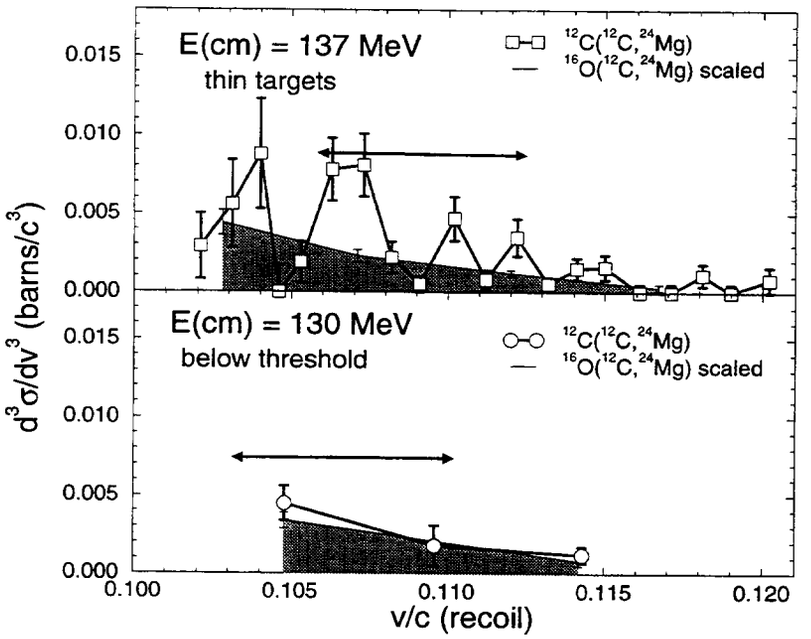

Figure 5. Galilean-invariant cross sections as a function of recoil velocity, obtained from measurements of the ^{12}C(^{12}C,^{24}Mg) reaction with a 486-μg/cm^2 target. Measurements were made at E_{cm} = 137 MeV (squares, top) and below absolute threshold at E_{cm} = 130 MeV (circles, bottom). Notation and backgrounds as in Fig. 4

lines in Fig. 4), based on the shape of the ^{25}Mg spectrum, may better represent the low-velocity increase for still heavier contaminants; within the "allowed" velocity range, the two background methods agree within 30 picobarns.

Additional Measurements

Forward-backward peaking in the pion distributions, observed in inclusive measurements at higher energies[16], is seen as a symmetric structure with a central valley in the π^+ channel (Fig.4, top), but is not visible in the neutral channel (Fig.4, bottom), where higher energy losses and final-state gamma emission broaden the velocity structures. Experiments with thinner (486 μg/cm^2) targets were performed to demonstrate that the π^0channel (Fig. 5, top) displays the same properties.

A measurement below the pion production threshold was performed to test whether the mass-24 yield originates from a radiative capture mechanism. The lower half of Fig. 5 shows the yield for the ^{12}C(^{12}C,^{24}Mg) channel just below threshold. The measured value at E_{cm} = 130 MeV is 59 $\pm$ 109 picobarns. Though this is consistent with zero, it cannot conclusively exclude contibutions of radiative capture processes to the ^{24}Mg yield, due to poor counting statistics. However, statistical-model calculations[17] predict cascade gamma deexcitation to be 3 orders of magnitude lower than the measured cross sections. As mentioned, single-photon processes are excluded kinematically. In the charged-pion channel, the issue does not arise, since ^{24}Na cannot be produced in the radiative capture reaction.

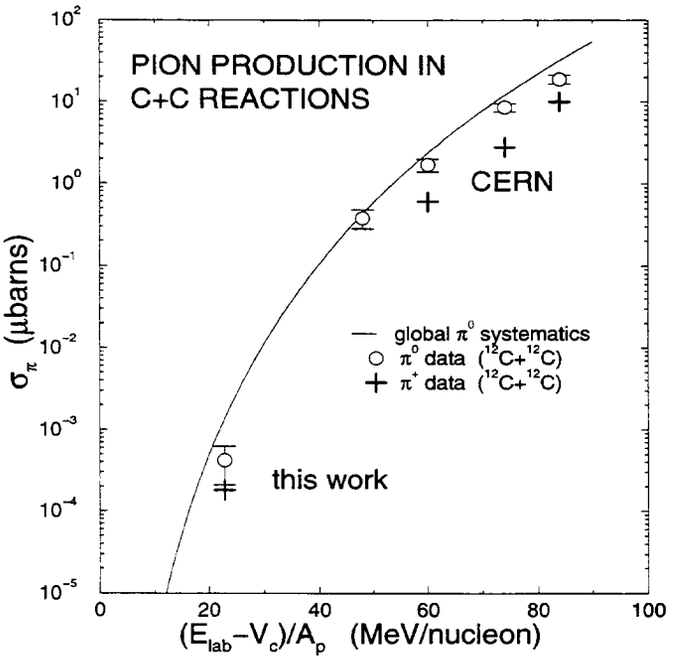

Figure 6. Systematics of π^0 and π^+ production in $^{12}C+^{12}C$ reactions. Low-energy π^0 point is taken as twice the $^{12}C(^{12}C,^{24}Mg)$ cross section.

DISCUSSION

The background-subtracted $^{12}C(^{12}C,^{24}Na)\pi^+$ and $^{12}C(^{12}C,^{24}Mg)\pi^0$ cross sections, including the additional thin-target data, are 182 ± 84 and 208 ± 38 picobarns, respectively, at E_{cm} = 137 MeV. The ^{24}Na cross section is representative of the entire π^+ production cross section, since excited states in the fusion residue cannot decay by nucleon or cluster emission. The π^0 production, however, must be greater than implied by the ^{24}Mg cross section, since the upper range of accessible levels in the residue are particle-unbound. A calculation including the specific T=1 levels available, their particle decay widths, and associated phase space factors indicates that about half the residues should survive; in comparisons with the systematics of heavy-ion π^0 production, we therefore give the range as one to three times the measured $^{12}C(^{12}C,^{24}Mg)\pi^0$ cross section.

The pion yield for $^{12}C+^{12}C$ reactions is given in Fig. 6. The solid curve is a power-law fit to tabulated π^0 data[6] with total system mass less than 100. Higher-energy data are from work at CERN[16, 18]. Our results are consistent with an extrapolation of the higher-energy inclusive data. The extension of the pion-production excitation function to low energies permits discussion of the range of validity for various models. The incoherent summation of on-shell nucleon-nucleon collisions[1], though applicable for higher energies, does not reproduce our results. Similarly, the pionic bremsstrahlung model[9] is inappropriate for our near-threshold results, since it rquires $E_{cm} \geq m_\pi c^2 + E_{Coul}$. After the relatively gentle deceleration from the Coulomb barrier, insufficient kinetic energy remains to produce a pion; the potential energy of fusion should not contribute through this mechanism. Thermal and statistical models [6, 10] should be testable by our data since, in contrast with inclusive measurements, pionic fusion defines the size and excitation of the emitting volume and the "daughter state" of the residue. Finally, microscopic models[12] would require a two-step (or two-nucleon) process to

conserve isospin with our T=0 entrance channel; the pionic fusion of two heavy ions requires this process to be further off shell than do proton-induced reactions.

SUMMARY

We have measured the $^{12}C(^{12}C,^{24}Mg)\pi^0$ and $^{12}C(^{12}C,^{24}Na)\pi^+$ cross sections at E_{cm} = 137 MeV to obtain 208±38 and 182±84 picobarns, respectively. This constitutes the first experimental observation of the pionic fusion of heavy ions. Observation of this phenomenon so near threshold places additional constraints on the production mechanisms, requiring that they incorporate the kinetic energy of the entire 24-nucleon system as well as the binding energy gained in fusion.

REFERENCES

1. W. Cassing *et al.*, Phys. Rep. **188** (1990) 363.
2. Peter Braun-Munzinger and Johanna Stachel, Ann. Rev. Nucl. Part. Sci. **37** (1987) 97, and references therein.
3. Y. Le Bornec *et al.*, Phys. Rev. Lett. **47** (1981) 1870.
4. L. Bimbot *et al.*, Phys. Rev. **C30** (1984) 739.
5. W. Schott *et al.*, Phys. Rev. **C34** (1986) 1406.
6. M. Prakash *et al.*, Phys. Rev. **C33** (1986) 937.
7. G.R. Young *et al.*, Phys. Rev. **C33** (1986) 742.
8. G.F Bertsch *et al.*, Phys. Rev. **C15** (1977) 713.
9. D. Vasak *et al.*, Nucl. Phys. **A428** (1984) 291c.
10. L. Potvin *et al.*, Phys. Rev. **C38** (1988) 2964.
11. Harold W. Fearing, in *Pion Production and Absorption in Nuclei - 1981*, AIP Conference Proceedings **79** (1982).
12. L. Harzheim *et al.*, Z. Phys. **A340** (1991) 399.
13. J.C.D. Milton *et al.*, Atomic Energy of Canada Internal Report AECL-3563 (1970).
14. G.C. Ball *et al.*, Nucl. Phys. **A325** (1979) 305 and D. Horn *et al.*, PR-TASCC-9: 3.1.10; AECL-11239.
15. J.S. Forster *et al.*, TASCC-P-95-28 and Nucl. Inst. and Meth. **B**, in press.
16. E. Grosse, Nucl. Phys. **A447** (1985) 611c.
17. M. Chadwick (private communication).
18. V. Bernard *et al.*, Nucl. Phys. **A423** (1984) 411.